Accelerated biofluid filling in complex microfluidic networks by vacuum-pressure accelerated movement (V-PAM)

Zeta Tak For Yu[a], **Mei Ki Cheung**[a], **Shirley Xiaosu Liu**[a], and **Jianping Fu**[a,b,c,d,*]

[a]Department of Mechanical Engineering, University of Michigan, Ann Arbor, Michigan 48109, USA

[b]Department of Biomedical Engineering, University of Michigan, Ann Arbor, Michigan 48109, USA

[c]Department of Cell and Developmental Biology, University of Michigan Medical School, Ann Arbor, MI 48109, USA

[d]Michigan Center for Integrative Research in Critical Care, University of Michigan, Ann Arbor, MI 48109, USA.

Abstract

Rapid fluid transport and exchange are critical operations involved in many microfluidic applications. However, conventional mechanisms used for driving fluid transport in microfluidics, such as micro-pumping and high pressure, can be inaccurate and difficult for implementation for integrated microfluidics containing control components and closed compartments. Herein we developed a technology termed Vacuum-Pressure Accelerated Movement (V-PAM) capable of significantly enhancing biofluid transport in complex microfluidic environments containing dead-end channels and closed chambers. Operation of the V-PAM entailed a pressurized fluid loading into microfluidic channels where gas confined inside could rapidly be dissipated through permeation through a thin, gas-permeable membrane sandwiched between microfluidic channels and a network of vacuum channels. We systematically studied effects of different structural and operational parameters of the V-PAM for promoting fluid filling in microfluidic environments. We further demonstrated the applicability of V-PAM for rapid filling of temperature-sensitive hydrogels and unprocessed whole blood into complex irregular microfluidic networks such as microfluidic leaf venation patterns and blood circulatory systems. Together, the V-PAM technology provides a promising generic microfluidic tool for advanced fluid control and transport in integrated microfluidics for different microfluidic diagnosis, organs-on-chips, and biomimetic studies.

INTRODUCTION

Even though fluid transport, incubation, and exchange are the most common operations involved in microfluidic assays, it remains a significant technical hurdle for rapid and accurate loading and manipulation of biofluids in integrated microfluidics containing numerous control components and closed reaction compartments.[1–4] Recent advances of

[*]Corresponding author (jpfu@umich.edu).

Organs-on-chips and microfluidic devices for blood analysis and tissue engineering applications have set up additional requirements for designs of intricate microfluidic networks connecting different functional components and filling of viscous biofluids containing human cells and room-temperature curable hydrogels in microfluidic networks. [5–6] Mammalian cells can be fragile and inherently sensitive to shear stress;[7–8] thus loading and manipulation of mammalian cells in microfluidic environments require extra care and consideration to avoid significant perturbations that could change cellular behaviors (or phenotypes) under study.[9–11] It is also known that clogging of microfluidic networks often arises when a viscous biofluid containing a dense amount of cellular or acellular components encounters a narrow microfluidic passage.[6,12–13]

Although some common practices have been implemented in the microfluidics field to transport biofluids rapidly in confining microfluidic environments, they suffer from various issues and thus have limited applicability. For example, loading liquids using micropumps has been commonly implemented in integrated microfluidics involving chemical reactions. [14–16] However, in practice, metering accuracy and evenness over multiple structures using micropumps have been highly susceptible to variations of microfluidic structural dimensions, flow resistance, and back pressure.[4,15] While filling biofluids in microfluidic devices containing dead-end channels and closed chambers can also be achieved by gas removal leveraging gas solubility and permeability properties of polydimethylsiloxane (PDMS), the material most commonly used in microfluidic devices, however, gas permeation rate through PDMS is low even at a moderate back pressure.[4,17] Making use of gas compressibility to instantaneously load biofluids in microfluidic devices by high pressure and vacuum has also been demonstrated recently.[18] However, in addition to imposing stringent criteria on experiential setup and chip construction and operation, high pressure operation can lead to large shear stresses that can have deleterious effects on certain biological entities such as mammalian cells.[19]

While pressure has been the prevailing force in pneumatic microfluidics, its complementary force, vacuum, has found less applications in microfluidic operations. Besides used as a degassing module for microfluidics,[20–22] vacuum-based degassing has recently been exploited as a pumping mechanism for controlling fluid transport in point-of-care (POC) microfluidic devices.[23–25] Vacuum can also indirectly control or pump fluids in microfluidic devices through a gas-permeable PDMS membrane.[26–30] Although these previous studies have provided an important foundation and proof that vacuum can be incorporated into microfluidic device designs to facilitate transport and filling of fluids in microfluidic channels, only simple microfluidic configurations and applications have been reported so far. Thus the full potential of vacuum-based fluid transport in microfluidics awaits for exploration.

Herein, we studied and exploited the synergistic driving power of pressure and vacuum for achieving rapid filling of viscous biofluids in large-area, intricate, and confining microfluidic environments containing dead-end channels and closed chambers. We term the technology Vacuum-Pressure Accelerated Movement, or V-PAM, to signify the vacuum force acting on a gas-permeable PDMS membrane underneath a pressurized microfluidic channel to effectively enhance movement and thus filling of biofluids in microfluidic

environments (Fig. 1a). We systematically studied the effects of different structural and operational parameters of the V-PAM technology for promoting fluid filling in microfluidic environments. Given the importance of complex, irregular geometries and different biofluids used in Organs-on-chips and microfluidic devices for blood analysis and tissue engineering applications, in this work we further examined the applicability of V-PAM for rapid filling of complex biofluids (such as temperature-sensitive hydrogels and unprocessed whole blood) into complex irregular networks such as microfluidic leaf venation patterns and blood circulatory systems. Together, this work has demonstrated the V-PAM technology a generic microfluidic module for advanced fluid control and transport in integrated microfluidics for different microfluidic diagnosis, organs-on-chips, and biomimetic studies.

METHODS AND MATERIALS

Chip fabrication.

Microfluidic chips integrated with V-PAM were fabricated as described previously.[4,15,17] Briefly, original photos and images of complex pictorial patterns were first converted into CAD files (AutoCAD, Autodesk, Inc., San Rafael, CA) with a minimum feature size of 10 μm. CAD designs were processed and printed out as transparency masks by CAD/Art Services, Inc. (Bandon, OR). Two Si wafers were fabricated as flow layer and control layer molds using photolithography. For the flow layer Si mold, a two-layered photoresist structure was generated by applying photolithography twice. The first layer, about 20 – 40 μm thick, was patterned using negative photoresist, SU8 (Microchem, Westborough, MA). The second photoresist layer, made from a positive photoresist AZ50XT (Capitol Scientific, Austin, TX), was about 20 – 30 μm thick and was rounded using thermal reflow treatment at 130 °C for 20 – 30 min. The control layer Si mold contained a 30 – 50 μm thick SU8 layer containing control as well as vacuum channels for V-PAM. The two Si wafers were further coated conformally with 0.5 – 1 μm thick Parylene C dielectric layers at 690 °C and 30 mTorr (Specialty Coating Systems, Indianapolis, IN).

Microfluidic chips integrated with V-PAM were fabricated using the two Si molds by soft lithography.[4,15,17] For fabrication of flow layers, a 5 mm thick polydimethylsiloxane (PDMS; Dow Corning, Ellsworth, Germantown, WI) with a 10:1 monomer to curing agent ratio was poured over the flow layer Si mold, degassed, cured at 80 °C for 30 min, and peeled off from the flow layer Si mold. For fabrication of control layers, PDMS with a 20:1 monomer to curing agent ratio was spin-coated on the control layer Si mold at a spin speed between 1.6 – 4.5 krpm before baking at 80 °C for 30 min. Thickness of gas-permeable PDMS membranes was controlled by PDMS spin coating speed, with faster spin speed resulting in thinner gas-permeable PDMS membranes. PDMS flow layers were first cut into dices before they were cleaned, treated with air plasma (Femto Science, Gyeonggi-Do, Korea), and bonded to PDMS control layers under careful alignment with a custom-built desktop aligner.[31] After baking at 80 °C for 30 min, irreversibly bonded PDMS stacks were peeled off from the control Si mold and hole-punched. PDMS stacks were treated with air plasma before bonding onto a glass slide pre-coated with PDMS of a 10:1 monomer to curing agent ratio. PDMS microfluidic chips were further baked at 80 °C overnight to complete PDMS polymerization and strengthen bonding at interfaces between PDMS layers.

For control microfluidic chips without V-PAM, PDMS flow layers molded from the flow layer Si mold were directly bonded to glass slides with air plasma.

Microfluidic control.

An external pressure source, an electronic system, and control software were used to operate microvalves integrated into microfluidic chips.[4] In-house compressed air was filtered and regulated to provide pressure for overall control of microvalve operations. Pressure between 25 – 40 psi was used to actuate microvalve closure. The electronic system, composed of a voltage generator (National Instruments, Austin, TX) with output signals connected to a set of electrically addressable pneumatic valves and regulators (Festo, Arlington Heights, IL and SMC, H.H. Barnum, Brighton, MI), was used to actuate pressure supply to individual channels. LabVIEW (National Instruments) was programmed to regulate voltage generation. Compressed air and an in-house vacuum supply were used to generate static pressure and vacuum inside microfluidic chips, respectively. Alternatively, vacuum was also generated by a vacuum generator, which was calibrated by a vacuum gauge (both from McMaster-Carr, Cleveland, OH) using compressed air.

Biofluid samples.

A human promyeloblast cell line HL-60 (ATCC, Manassas, VA) derived from an acute promyelocytic leukemia patient was used. Culture medium comprised the basal medium IMDM (Life Technologies, Grand Island, NY) and 20% fetal bovine serum (FBS; Fisher Scientific, Pittsburgh, PA). Suspensions of single HL-60 cells were maintained in T75 tissue culture flasks at 37 °C and 5% CO_2 and were passaged every 3 – 4 days. HL-60 cells were stained fluorescently with 0.1 – 1% (v/v) Hoechst 33342 (Life Technologies, Grand Island, NY) for 5 min at room temperature before used in experiments. Suspensions of stained HL-60 cells were centrifuged before supernatant was removed. Known quantities of fluorescently labeled HL-60 cells were then spiked into either cell culture medium or undiluted healthy human whole blood. Blood collection process was approved by the Institutional Review Board (IRB) of the University of Michigan, Ann Arbor. Informed consents were obtained from healthy donors before blood collection. Briefly, fresh blood was collected into blood collection tubes pre-coated with anticoagulant EDTA. Blood samples were vortexed to avoid sedimentation and were used within 4 hr of blood collection. Matrigel (BD, Franklin Lakes, NJ) stored at −20 °C was first thawed to liquid at 4 °C in a refrigerator before use. It was kept on ice to avoid gelation till loaded into microfluidic chips. All biofluid filling experiments were conducted at room temperature.

Imaging and analysis.

Dynamics of biofluid filling in microfluidic chips was recorded using an imaging setup comprising a handheld digital microscope and a backlight illumination pad (both from Dino-Lite, SunriseDino, Hicksville, NY). Through imaging analysis, biofluid filling distance along microfluidic channels was obtained as a function of filling time. Bright field and fluorescence images showing fluorescently labeled HL-60 cells were recorded using a fluorescence microscope (AXIO Observer.Z1) attached with a CCD camera (AxioCam MRm), before the images were processed and stitched into a mosaic by software AxioVision

V4.8 (all from Carl Zeiss Microscopy, LLC, Thornwood, NY). Statistical analysis was based on independent experiments with $n \quad 3$.

RESULTS AND DISCUSSION

Principle and design of V-PAM technology

Leveraging the intrinsic gas solubility and permeability properties of PDMS, herein we developed a technology termed vacuum-pressure accelerated movement (V-PAM) to accelerate biofluid filling in complex microfluidic networks, including dead-end microfluidic channels. In V-PAM, a thin, gas-permeable PDMS membrane with a controlled thickness was sandwiched between a top PDMS flow layer with dead-end microfluidic channels to be filled with biofluids and a bottom PDMS control layer with a network of vacuum channels (Fig. 1a). Gas penetration through PDMS can be described using $N = p \times$ P / T, where N is the gas flux, p is the gas permeability coefficient, P is the pressure difference across the PDMS membrane, and T is the PDMS membrane thickness. Thus, steady-state gas flow rate across the degassing thin PDMS membrane is linearly proportional to total pressure difference across the PDMS membrane and its surface area and inversely proportional to PDMS membrane thickness.[27] Thus, in addition to vacuum applied to vacuum channels in the bottom control layer, a positive pressure was applied to microfluidic channels in the top flow layer to increase pressure difference across degassing PDMS membranes. Such sandwiched, layered construction of the V-PAM module enabled high gas flow rates across thin PDMS membranes and thus rapid biofluid filling in dead-end microfluidic channels. As PDMS thin membranes are elastic, large pressure differences across PDMS membranes could lead to significant deformation and extension of PDMS membranes, potentially resulting in collapse and stiction of PDMS membranes to vacuum channels. Thus, in V-PAM, support pillars were included in vacuum channels to alleviate PDMS membrane deformation (Fig. 1b).

To demonstrate effect of V-PAM on accelerating biofluid filling in microfluidic devices, straight, dead-end microfluidic channels integrated with or without V-PAM were filled with dye solutions under constant pressures applied to microfluidic channel inlets (Fig. 1c). Comparing time-course images recorded for microfluidic channels with or without V-PAM clearly revealed a dramatic effect of V-PAM on accelerating biofluid filling in dead-end microfluidic channels. For microfluidic channels bonded directly to cover glasses (negative control), it took more than 10 min to completely fill dead-end, straight microfluidic channels with a 1 cm length (the total channel filling time > 10 min). In distinct contrast, it took only 40 s to completely fill the same dead-end microfluidic channels when V-PAM was embedded beneath the entire microfluidic channels (100% V-PAM embedment), a 10-fold reduction of total filling time compared to negative control. To elaborate further on fluid filling dynamics, fluid filling distance was plotted against time for dead-end microfluidic channels integrated with or without V-PAM (Fig. 1d). In negative control without V-PAM, fluid filling in dead-end microfluidic channels continuously decelerated, presumably due to decreasing gas-permeation PDMS surface areas (Fig. 1d). In contrast, such decreasing gas-permeation PDMS area during fluid filling in dead-end microfluidic channels had a very insignificant effect on fluid filling for dead-end microfluidic channels implemented with

100% V-PAM embedment. This is understandable as V-PAM provided a low-resistance gas-permeation path toward vacuum channels in the bottom PDMS control layer. Fluid filling speed remained high throughout the entire biofluid filling process for dead-end microfluidic channels integrated with V-PAM (Fig. 1d).

Control parameters of V-PAM technology

To optimize V-PAM technology, several V-PAM structural parameters, including vacuum channel length L, support pillar separation distance D (Fig. 2), and PDMS membrane thickness (controlled by PDMS spin-coating speed S), were studied to examine their independent effects on accelerating biofluid filling in straight, dead-end microfluidic channels. Figure 3a plots the time needed for completely filling 1 cm-long, straight, dead-end microfluidic channels as V-PAM vacuum channel lengths varied from 0 – 1 cm, corresponding to 0% - 100% V-PAM embedment from the end of microfluidic channels. Surprising, even with only 10% V-PAM embedment, a 10-fold reduction of the total filling time was achieved compared to negative control, where the total filling time was > 10 min. The total filling time continued to decrease to about 25 s as V-PAM vacuum channel length increased to 1 cm and thinner PDMS membranes were used. It should be noted that even when a blank PDMS membrane without vacuum channels were used in the bottom PDMS control layer (0% V-PAM embedment), fluid filling was also significantly accelerated (by about 2 folds) comparing to negative control.

V-PAM modules integrated with support pillars of various separation distances were compared for their effects on accelerating fluid filling in 1 cm-long, straight, dead-end microfluidic channels (Fig. 3b). Counter-intuitively, smaller support pillar separation distances, which effectively reduced gas-permeation PDMS surface areas, led to faster fluid filling in microfluidic channels with 100% V-PAM embedment (Fig. 3b). This trend was consistent for V-PAM modules with different degassing PDMS membrane thicknesses (Fig. 3b). Lastly, the total filling time for straight, dead-end microfluidic channels decreased with decreasing PDMS membrane thickness (or increasing PDMS spin-coating speed S), regardless of separation distances between support pillars in V-PAM modules (Fig. 3c).

Even with support pillars embedded in vacuum channels, due to its elasticity, thin degassing PDMS membranes would unavoidably deform and even collapse and stick to the floor of vacuum channels under significant pressure difference across the PDMS membrane. With increasing support pillar separation distance, it was observed that support pillars and PDMS membranes went through several deformation states: (i) bending of support pillars (Fig. 4a, *left*), (ii) deformation and stiction of PDMS membranes to the floor of vacuum channels (Fig. 4a, *middle*), and (iii) severe collapse of PDMS membranes onto the vacuum channel floor, thus significantly reducing gas-permeation PDMS surface area leading to a state of "choke" (Fig. 4a, *right*). These observations were consistent with the experimental data in Fig. 3b, where smaller support pillar separation distances led to faster fluid filling in dead-end microfluidic channels.

With V-PAM actuated, the thickness of degassing PDMS membranes had a significant effect on the extent of its deformation and collapse onto the vacuum channel floor. As expected, thinner degassing PDMS membranes led to more severe deformation and stiction of PDMS

membrane to the floor of vacuum channels (Fig. 4b). Interesting, as thinner PDMS membranes could enhance gas permeation across the PDMS membrane, it appeared that the benefit of reducing the thickness of degassing PDMS membranes outweighed its negative effect on decreased PDMS penetration surface area. Thus, as observed in Fig. 3c, the total filling time for dead-end microfluidic channels decreased with decreasing PDMS membrane thickness (or increasing PDMS spin-coating speed).

V-PAM technology applied to complex irregular networks

To further demonstrate its utility for accelerating biofluid filling in complex microfluidic networks with dead-end channels, the V-PAM module was applied to large-area microfluidic structures including a microfluidic leaf venation pattern (1 cm × 1 cm; Fig. 5a&b) and a microfluidic blood circulatory system (the "µMan" chip, 0.45 cm × 1.2 cm; Fig. 5d&e). Both microfluidic structures contained complex vascular networks of veins / branches and dead-end channels with a minimum channel width of 10 µm. These microfluidic structures have been employed by previous studies to examine tissue constructs with significant applications in organs-on-chips and tissue engineering.[33] Standard methods to fill in solutions in these complex microfluidic networks often lead to bubble cavitations and slow filling processes due to high flow resistance resulted from surface tension, flow viscosity, and dead-end channels.[17] Filling of dye solutions in these large-area microfluidic structures was significantly accelerated when V-PAM module was integrated with the microfluidic structures. Specifically, filling of the leaf vascular network with dye solutions under V-PAM activation was accomplished within 20 s (Fig. 5c). By integrating microvalves into the microfluidic blood circulatory system design, two dye solutions entered the circulatory system from both palms, and complete filling of the µMan chip was accomplished with 3 s (Fig. 5f). Since filling of the µMan pattern was completed within a very short period of time, diffusion between dyes within the microfluidic blood circulatory system was minimal (Fig. 5f).

V-PAM technology applied to temperature- and time-sensitive biofluids

Extracellular matrix (ECM) is a critical environmental factor that can affect and control cell structures and behaviors.[34] In many microfluidic systems designed for stem cell culture and tissue engineering applications, ECM proteins need to be pre-loaded into microfluidic channels to properly control cell-ECM interactions. Among these ECM proteins, Matrigel is one of the most commonly used gelatinous protein mixtures. However, due to its curability at room temperature, rapid filling of Matrigel solutions into microfluidic channels evenly and without bubble formation can be difficult. Thus, to extend the utility of V-PAM to filling hydrogel solutions in microfluidic structures, Matrigel solutions were loaded into straight, 1-cm long, dead-end microfluidic channels integrated with or without V-PAM modules at room temperature (Fig. 6a). For negative control without V-PAM, it took more than 1,100 s to completely fill Matrigel solutions in the microfluidic channels. Quantitative analysis of channel filling distance as a function of filling time revealed that filling speed of Matrigel solutions dropped very rapidly during the filling process, and it took almost 2/3 of the total filling time just to fill the last 20% of channel length, supporting an exacerbated difficulty associated with highly viscous and gelling hydrogel solutions in filling microfluidic channels at room temperature (Fig. 6b). In distinct contrast, V-PAM implementation

significantly accelerated filling of Matrigel solutions in dead-end microfluidic channels, and complete channel filling was accomplished within just about 50 s. Rapid filling of Matrigel solutions under V-PAM activation also ensured them to stay in a liquid form, leading to a constant filling speed throughout the entire filling process (Fig. 6b). Figure 6c demonstrated that filling Matrigel solutions in dead-end microfluidic channels with V-PAM implementation was largely unaffected by separation distance of support pillars employed in the V-PAM module.

We further employed the V-PAM module to speed up filling of hydrogel solutions in the microfluidic leaf venation pattern. Careful examinations of the vascular network in the leaf venation pattern without V-PAM revealed that in 10 s, only major branches of the vascular network were filled with Matrigel solution (Fig. 6d, *middle left*), in distinct contrast to the V-PAM-embedded microfluidic leaf venation pattern that was completely filled within 10 s (Fig. 6d, *top right*). We should note that for filling the microfluidic leaf venation pattern with Matrigel solutions without the V-PAM module, we had to cool down the microfluidic setup using ice. With microvalves or micropumps, multiple hydrogel solutions can be loaded into the leaf venation pattern in parallel or in series. An example of loading two gel solutions in parallel into the leaf venation was demonstrated in this work (Fig. 4d, *bottom*), suggesting the feasibility of integrating both V-PAM and microfluidic spatial-temporal controls into single technological platforms.

V-PAM technology applied to cellular suspensions

Microfluidic devices are well suited for blood-based diagnosis given their precise control over the cell microenvironment and the ability to scale down analysis to very small volumes of blood.[6] However, clogging can be a critical issue when processing complex biofluids containing blood cells (especially unprocessed whole blood samples) using integrated microfluidics. To examine whether V-PAM could facilitate filling of blood samples in complex microfluidic structures, fluorescently labeled human leukemic HL-60 cells suspended in cell culture medium and undiluted human whole blood were first loaded into straight, 1-cm long, dead-end microfluidic channels with various widths comparable to those of arteriole, venule, and capillary (mean diameter: 8 – 30 μm). Using fluorescently labeled HL-60 cells allowed us to visualize cell distribution in confining microfluidic environments. The total filling time for the straight, dead-end channels was plotted in Fig. 7a. Due to a constant channel thickness, a smaller channel width and thus a greater surface-to-volume ratio led to a shorter total filling time (Fig. 7a). With V-PAM, the total filling time between channels of different widths for both cell culture medium and whole blood samples was very comparable and significantly less to those without V-PAM (about 10- to 40-fold improvements; Fig. 7a).

Ratio of total filling time for filling HL-60 samples in straight, dead-end microfluidic channels without and with V-PAM was plotted in Fig. 7b. Because of a higher cellular content and thus effective fluid viscosity, a greater effect from V-PAM to facilitate biofluid filling was observed for HL-60 spiked whole blood samples than culture medium suspensions. Importantly, V-PAM implementation also promoted uniform cell distribution in confining microfluidic channels, which was especially obvious for culture medium samples

spiked with HL-60 cells (Fig. 7c). Whereas without V-PAM, cell distribution could be rather heterogeneous in narrow microfluidic channels with critical dimensions comparable to cell size (Fig. 7c).

We further applied V-PAM to promote filling of fluorescently labeled HL-60 cells suspended in cell culture medium and undiluted human whole blood for the μMan chip. Filling the μMan with V-PAM was about 10-fold faster than without V-PAM, for both cell culture medium and whole blood samples (Fig. 7d). Similarly, cell distribution in the μMan chip with V-PAM was significantly more homogeneous than without V-PAM (**Fig. 7e**).

CONCLUSION

In this work, we integrated microfluidic circuit design and pressure-vacuum operation to develop and implement a versatile V-PAM technology for achieving rapid filling of viscous biofluids in large-area, intricate, and confining microfluidic environments containing dead-end channels and closed chambers. Microfluidic device designs containing dead-end channels and closed environments are common for applications such as immunoassays and cell-based assays.[4,17] The V-PAM technology eliminates high pressure required in conventional microfluidic operations for air removal in such microfluidic devices containing dead-end channels and closed environments. Furthermore, its applicability for rapid filling of complex biofluids (such as temperature-sensitive hydrogels and unprocessed whole blood) into complex irregular networks makes it an ideal operational module to be integrated into different microfluidic diagnosis, organs-on-chips, and biomimetic studies.

Implementing the V-PAM module would require researchers to have access to either pressure or vacuum resources. In addition to vacuum pumps, it is convenient to generate vacuum by other established methods.[33] In this work, we mainly used in-house vacuum, which is available in many research laboratories. Furthermore, we demonstrated in this work that in-house pressure could be used to generate vacuum as well by using a vacuum generator (see Methods and Materials). Finally, vacuum also can be generated through a syringe pulled manually or in conjunction to a syringe pump.[33]

Design and implementation of the V-PAM technology are versatile and compatible with different integrated microfluidic applications. Given that V-PAM was fabricated using soft-lithography, its integration with other PDMS-based microfluidic devices should be straightforward. Importantly, V-PAM regulation can be integrated with microvalve operations to achieve advanced flow control in microfluidics such as large-scale integration (LSI) and digital microfluidics, but with a higher operation speed, efficiency, and throughput. Unlike previous methods to promote biofluid filling in microchips by pre-treating devices through either surface chemistry or pre-vacuuming[23–25], which can be unstable and temporary, the V-PAM method is based on actively regulated gas transport through a thin, gas-permeable PDMS membrane, making its operation and performance more reliable and time-insensitive. Actuation of V-PAM is through vacuum channel connection and vacuum application. Thus, V-PAM implementation in microfluidic chips can easily achieve on-demand switching with precise spatial and temporal controls. We envision that in addition to promoting rapid filling of viscous biofluids in microfluidics, the V-PAM

technology can be further implemented in the future for other important microfluidic operations such as fluid mixing and droplet manipulation.

ACKNOWLEDGEMENTS

REFERENCES

[1]. Garcia-Cordero JL, Maerkl SJ, Lab Chip 2013, 14 (15), 2642–50. [PubMed: 24345965]

[2]. Lee CC, Sui G, Elizarov A, Shu CJ, Shin YS, Dooley AN, Huang J, Daridon A, Wyatt P, Stout D, Kolb HC, Witte ON, Satyamurthy N, Heath JR, Phelps ME, Quake SR, Tseng HR, Science 2005, 310 (5755), 1793–6. [PubMed: 16357255]

[3]. Thorsen T, Maerkl SJ, Quake SR, Science 2002, 298 (5593), 580–4. [PubMed: 12351675]

[4]. Yu ZT, Guan H, Cheung MK, McHugh WM, Cornell TT, Shanley TP, Kurabayashi K, Fu J, Sci. Rep. 2015, 5, 11339. [PubMed: 26074253]

[5]. Huh D, Hamilton GA, Ingber DE, Trends Cell Biol. 2011, 21 (12), 745–754. [PubMed: 22033488]

[6]. Yu ZT, Aw Yong KM, Fu J, Small 2014, 10 (9), 1687–703. [PubMed: 24515899]

[7]. Brindley D, Moorthy K, Lee JH, Mason C, Kim HW, Wall I, J Tissue Eng 2011, 2011, 620247. [PubMed: 21904661]

[8]. Lam RHW, Sun YB, Chen WQ, Fu JP, Lab Chip 2012, 12 (10), 1865–1873. [PubMed: 22437210]

[9]. Kamei K, Guo S, Yu ZT, Takahashi H, Gschweng E, Suh C, Wang X, Tang J, McLaughlin J, Witte ON, Lee KB, Tseng HR, Lab Chip 2009, 9 (4), 555–63. [PubMed: 19190791]

[10]. Kamei KI, Ohashi M, Gschweng E, Ho Q, Suh J, Tang JH, Yu ZTF, Clark AT, Pyle AD, Teitell MA, Lee KB, Witte ON, Tseng HR, Lab Chip 2010, 10 (9), 1113–1119. [PubMed: 20390128]

[11]. Gattazzo F, Urciuolo A, Bonaldo P, Biochim. Biophys. Acta 2014, 1840 (8), 2506–19. [PubMed: 24418517]

[12]. Chen W, Huang NT, Li X, Yu ZT, Kurabayashi K, Fu J, Front. Oncol. 2013, 3, 98. [PubMed: 23626950]

[13]. Toner M, Irimia D, Annu. Rev. Biomed. Eng. 2005, 7, 77–103. [PubMed: 16004567]

[14]. Unger MA, Chou HP, Thorsen T, Scherer A, Quake SR, Science 2000, 288 (5463), 113–6. [PubMed: 10753110]

[15]. Vu NT, Yu ZT, Comin-Anduix B, Sondergaard JN, Silverman RW, Chang CY, Ribas A, Tseng HR, Chatziioannou AF, J. Nucl. Med. 2011, 52 (5), 815–21. [PubMed: 21536929]

[16]. Studer V, Hang G, Pandolfi A, Ortiz M, Anderson WF, Quake SR, J. Appl. Phys. 2004, 95 (1), 393–398.

[17]. Yu ZT, Kamei K, Takahashi H, Shu CJ, Wang X, He GW, Silverman R, Radu CG, Witte ON, Lee KB, Tseng HR, Biomed. Microdevices 2009, 11 (3), 547–55. [PubMed: 19130244]

[18]. Liu K, Chen YC, Tseng HR, Shen CK, van Dam RM, Microfluid Nanofluidics 2010, 9 (4–5), 933–943. [PubMed: 20930933]

[19]. Hu W, Berdugo C, Chalmers JJ, Cytotechnology 2011, 63 (5), 445–60. [PubMed: 21785843]

[20]. Karlsson JM, Gazin M, Laakso S, Haraldsson T, Malhotra-Kumar S, Maki M, Goossens H, van der Wijngaart W, Lab Chip 2013, 13 (22), 4366–73. [PubMed: 24056885]

[21]. Johnson M, Liddiard G, Eddings M, Gale B, J Micromech Microeng 2009, 19 (9).

[22]. Lochovsky C, Yasotharan S, Gunther A, Lab Chip 2012, 12 (3), 595–601. [PubMed: 22159026]

[23]. Cira NJ, Ho JY, Dueck ME, Weibel DB, Lab Chip 2012, 12 (6), 1052–9. [PubMed: 22193301]

[24]. Monahan J, Gewirth AA, Nuzzo RG, Anal. Chem. 2001, 73 (13), 3193–7. [PubMed: 11467573]

[25]. Zhou X, Lau L, Lam WW, Au SW, Zheng B, Anal. Chem. 2007, 79 (13), 4924–30. [PubMed: 17547370]

[26]. Gao Y, Li P, Pappas D, Biomed. Microdevices 2013, 15 (6), 907–915. [PubMed: 23813077]

[27]. Eddings MA, Gale BK, J Micromech Microeng 2006, 16 (11), 2396–2402.

[28]. Chuang HS, Thakur R, Wereley ST, J Micromech Microeng 2012, 22 (8).

[29]. Somaweera H, Ibragimov A, Pappas D, Analyst 2013, 138 (19), 5566–71. [PubMed: 23939026]

[30]. Kolnik M, Tsimring LS, Hasty J, Lab Chip 2012, 12 (22), 4732–7. [PubMed: 22961584]

[31]. Li X, Yu ZTF, Geraldo D, Weng SN, Alve N, Dun W, Kini A, Patel K, Shu R, Zhang F, Li G, Jin QH, Fu JP, Rev. Sci. Instrum. 2015, 86 (7).

[32]. Chung BG, Park JW, Hu JS, Huang C, Monuki ES, Jeon NL, BMC Biotechnol 2007, 7, 60. [PubMed: 17883868]

[33]. He J, Mao M, Liu Y, Shao J, Jin Z, Li D, Adv. Healthc. Mater. 2013, 2 (8), 1108–13. [PubMed: 23554383]

[34]. Lukashev ME, Werb Z, Trends Cell Biol. 1998, 8 (11), 437–441. [PubMed: 9854310]

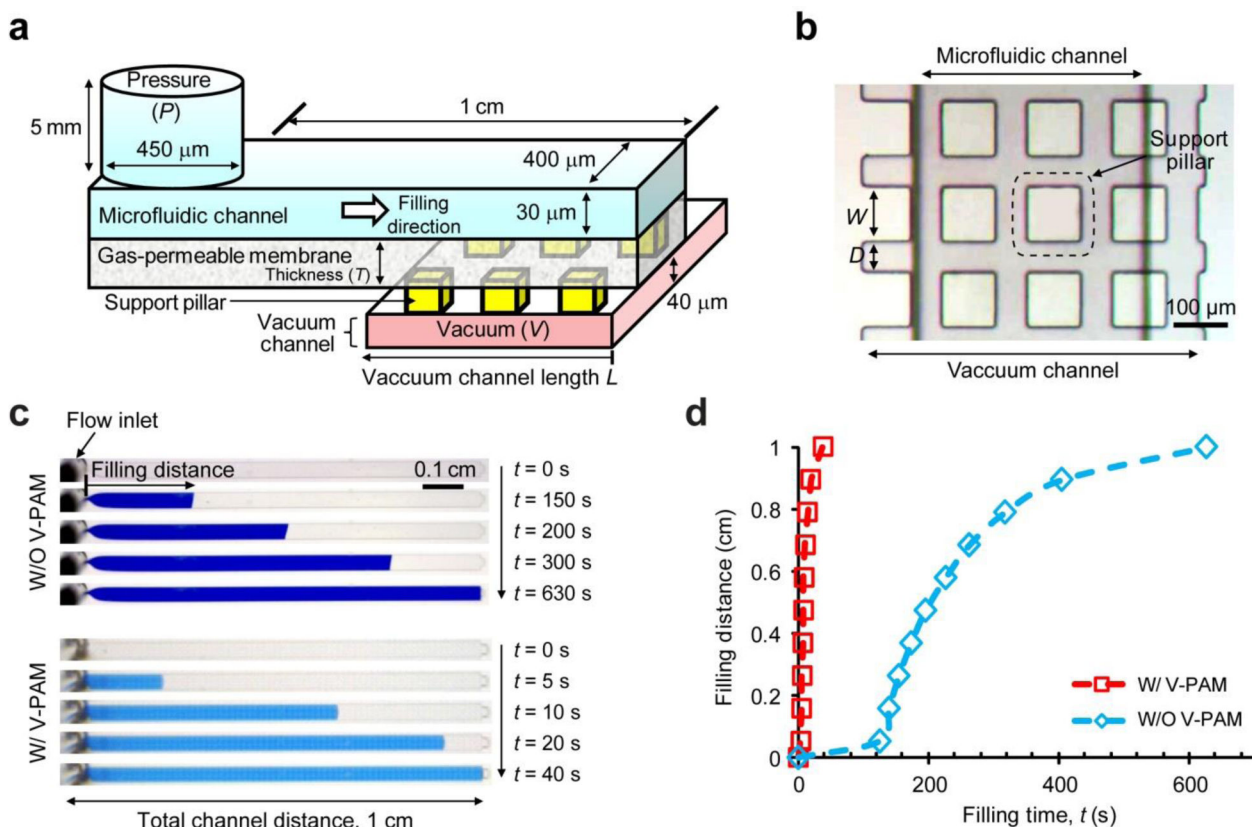**Figure 1.**
Principle and demonstration of vacuum-pressure accelerated movement (V-PAM) in microfluidic chips. (**a**) V-PAM module composed of a gas-permeable, thin PDMS membrane sandwiched between dead-end microfluidic channels to be filled with biofluid solutions and vacuum channels. A pressure (P) applied at the inlet of microfluidic channels drove liquid into the channel while pushing air trapped at the channel dead end to permeate through the PDMS membrane to the vacuum channel, where a vacuum (V) was maintained to enhance gas permeation through the PDMS membrane. (**b**) Top view of a microfluidic channel overlaid on top of a vacuum channel with the PDMS membrane sandwiched in between. To prevent deformation of PDMS membranes, an array of rectangular support pillars with a width of W and separated by a distance D was included in the vacuum channel. (**c**) Bright field images showing filling processes of dye solutions in straight, dead-end microchannels without (*top*) or with (*bottom*) V-PAM modules implemented. Images were recorded at different time points after the onset of the filling process ($t = 0$ s) as indicated. P: 12.5 psi, V: 12.5 psi, W: 100 μm, and D: 50 μm. Vacuum channel length (L) was the same as the length of microfluidic channels, *ca.* 1 cm. (**d**) Plot of fluid filling distance as a function of filling time t.
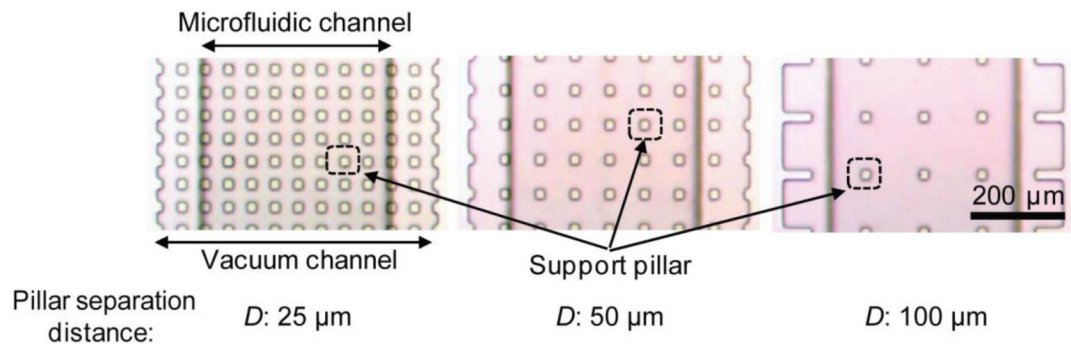
Figure 2.
Arrays of rectangular support pillars in vacuum channels with the same width W ($W = 25$ μm) but different separation distances D ($D = 25, 50, 100$ μm), as indicated.
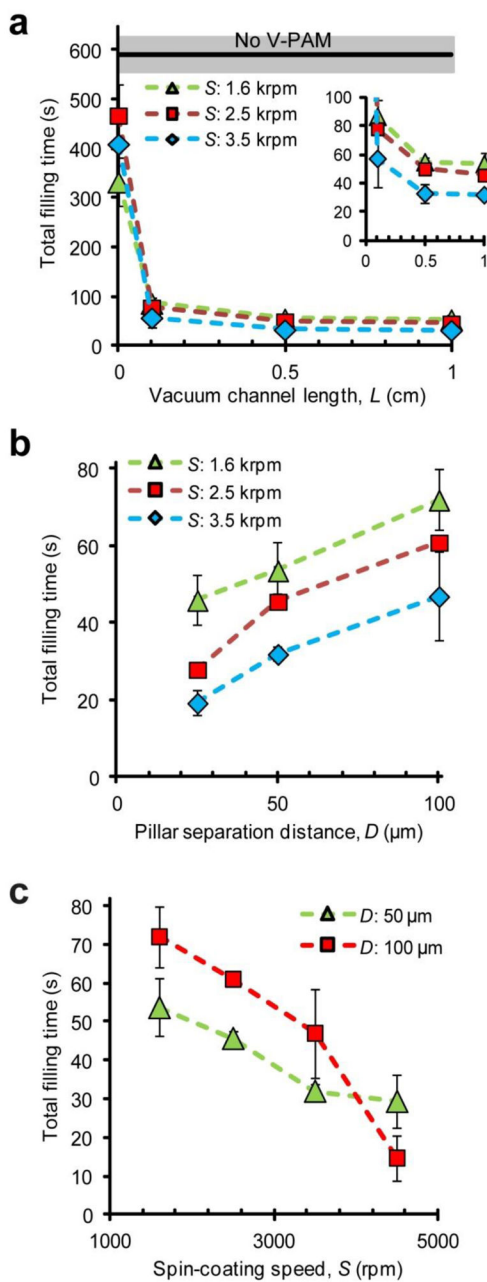
Figure 3.
Effects of V-PAM structural parameters on biofluid filling in 1 cm-long, straight, dead-end microfluidic channels. (**a**) Effect of vacuum channel length L on the time needed for filling entire microfluidic channels (the total filling time). Mean (*black line*) ± one standard deviation (S.D., *grey area*) of total filling time for microchannels without V-PAM was included for comparison. The inset showed data with L of 0.1 – 1 cm. D: 50 μm. (**b**) Plot of total filling time as a function of pillar separation distance D. L: 1 cm. (**c**) Plot of total filling time as a function of spin-coating speed S used for generating thin PDMS membranes. L: 1 cm. In all cases, P: 12.5 psi, V: 12.5 psi, and W: 25 μm.
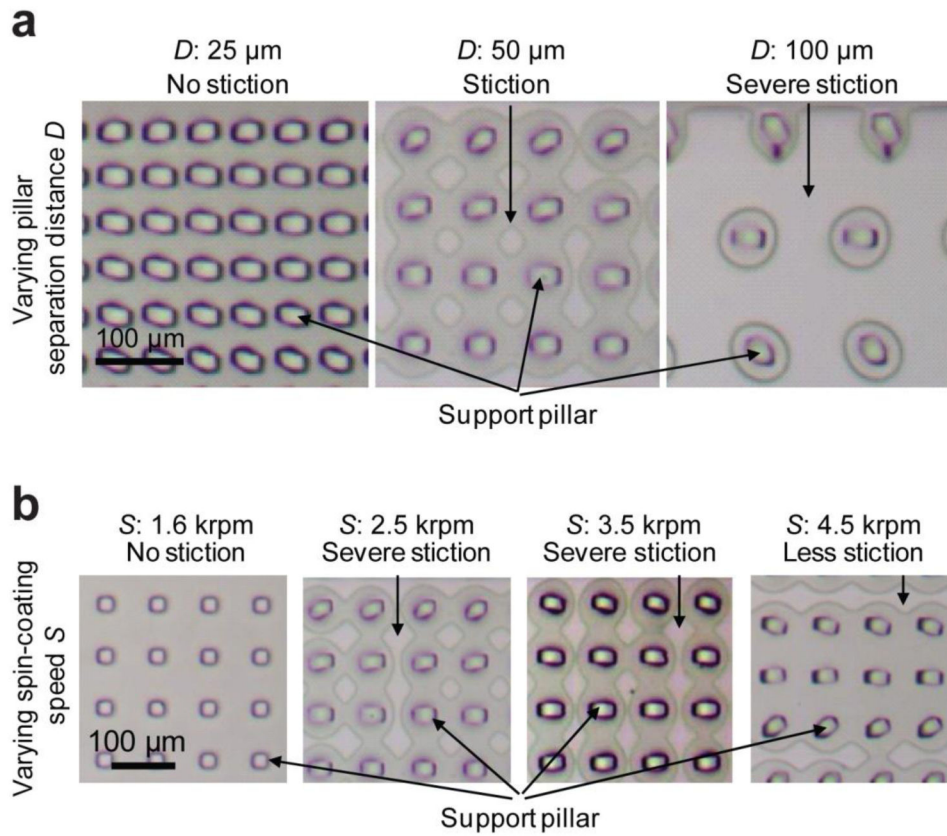
Figure 4.
Bright field images illustrating deformation and stiction of thin PDMS membranes to the bottom of vacuum channels when V-PAM was implemented. (**a**) shows representative images for support pillar arrays with the same width W but different separation distances D (D = 25, 50, 100 μm) as indicated. (**b**) shows representative images for thin PDMS membranes generated with different spin-coating speeds S as indicated. D: 50 μm. In all cases, P: 12.5 psi, V: 12.5 psi, and W: 25 μm.
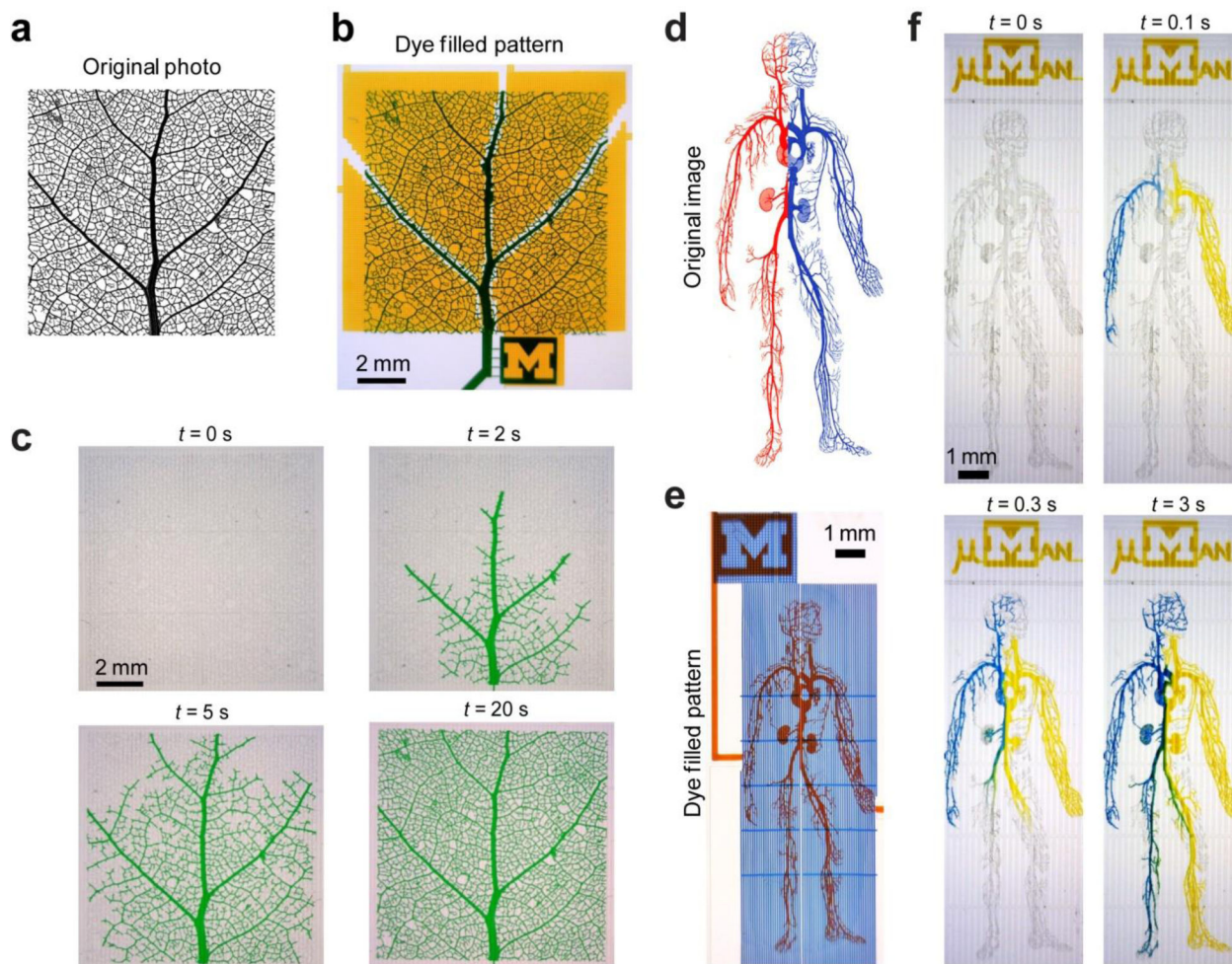
Figure 5.
V-PAM assisted rapid biofluid filling in irregular microfluidic geometries with dead-end channels. (**a**) Original photo of leaf venation. Photo permission of SmugMug, Inc. (**b**) Microfluidic leaf patterns and V-PAM vacuum channels were filled with *blue* and *maize* dye solutions, respectively, for visualization. (**c**) Bright field images showing rapid filling of a *green* dye solution in microfluidic leaf patterns with V-PAM activated. *P*: 2 psi. (**d**) Original image depicting the human blood circulation system. Note *red* and *blue* vessels correspond to arterial and venous systems, respectively. Image courtesy of the Access Excellence, National Health Museum. (**e**) Microfluidic human (μMan) chip filled with *red* and *blue* dye solutions to visualize the vessel and V-PAM pattern, respectively. (**f**) Bright field images showing rapid filling of the μMan chip with *blue* and *maize* solutions through two inlets at two palms. *P*: 12.5 psi. In all cases, *S*: 1.6 krpm, and *V*: 12.5 psi.
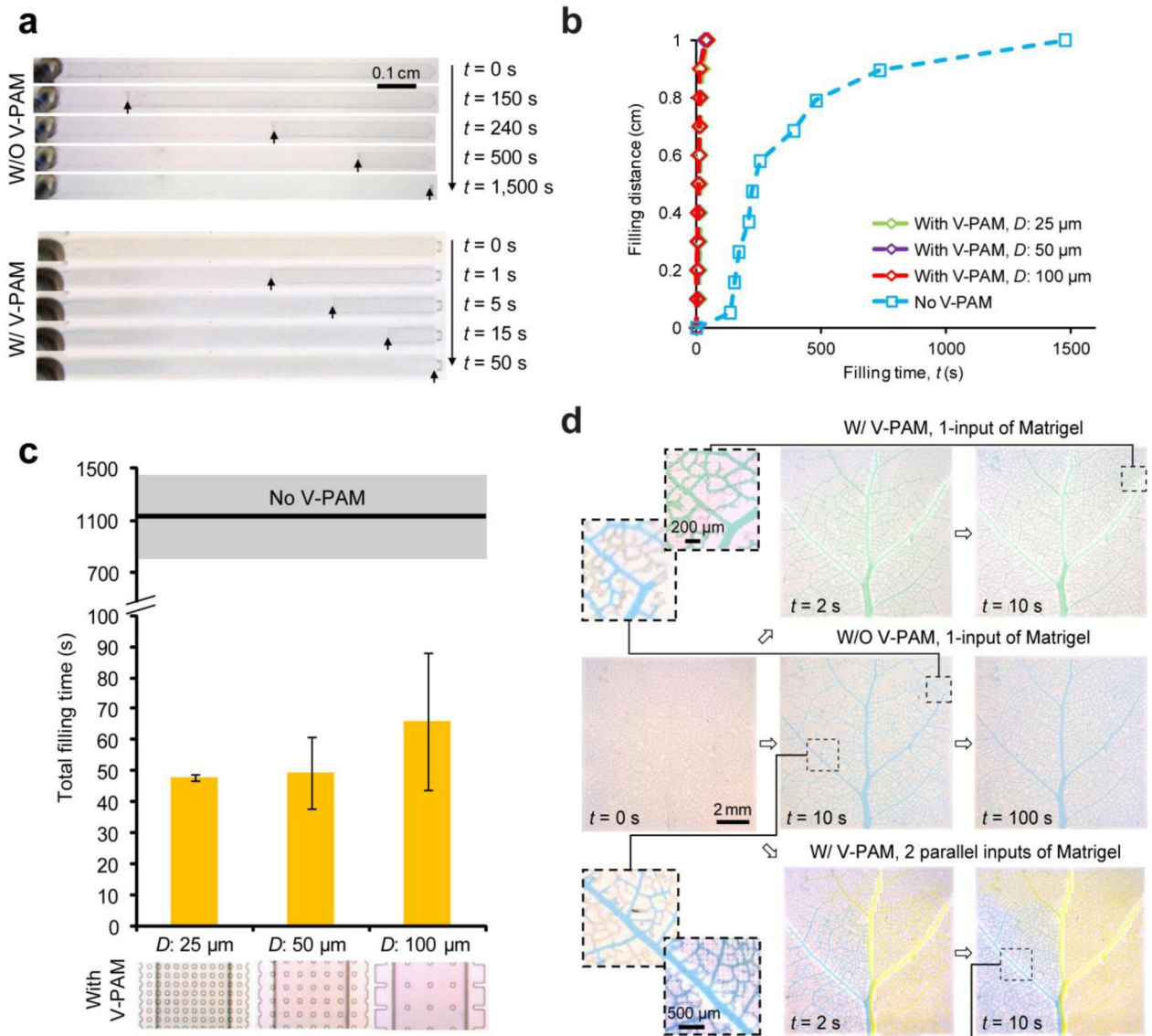
Figure 6.
Rapid filling of Matrigel solutions in microfluidic patterns with dead-end channels using V-PAM at room temperature (20 °C). (**a**) Bright field images showing filling of Matrigel solutions in straight, dead-end microchannels without (*top*) or with (*bottom*) V-PAM modules implemented. Images were recorded at different time points after the onset of the filling process ($t = 0$ s) as indicated. Arrows point to Matrigel solution fronts for easy visualization. For cases with V-PAM, *W*: 25 μm, *D*: 50 μm, and *L*: 1 cm. (**b**) Plot of Matrigel solution filling distance as a function of filling time *t*. (**c**) Comparison of total filling time between microchannels without or with V-PAM modules. V-PAMs with support pillar arrays of different separation distances *D* (*D* = 25, 50, 100 μm) were included. Mean (*black line*) ± S.D. (*grey area*) of total filling time for microchannels without V-PAM were included for comparison. (**d**) Bright field images showing leaf venation patterns filled with Matrigel solutions. 5% dyes were added to Matrigel for visualization. Paired zoom-in images were shown to compare filling of Matrigel solutions at the same leaf venation locations.

Microvalves (not shown in images) below the main leaf branch were used to drive gel solutions through either 1 input or 2 parallel inputs. In all cases, S: 1.6 krpm, P: 12.5 psi, and V: 12.5 psi.
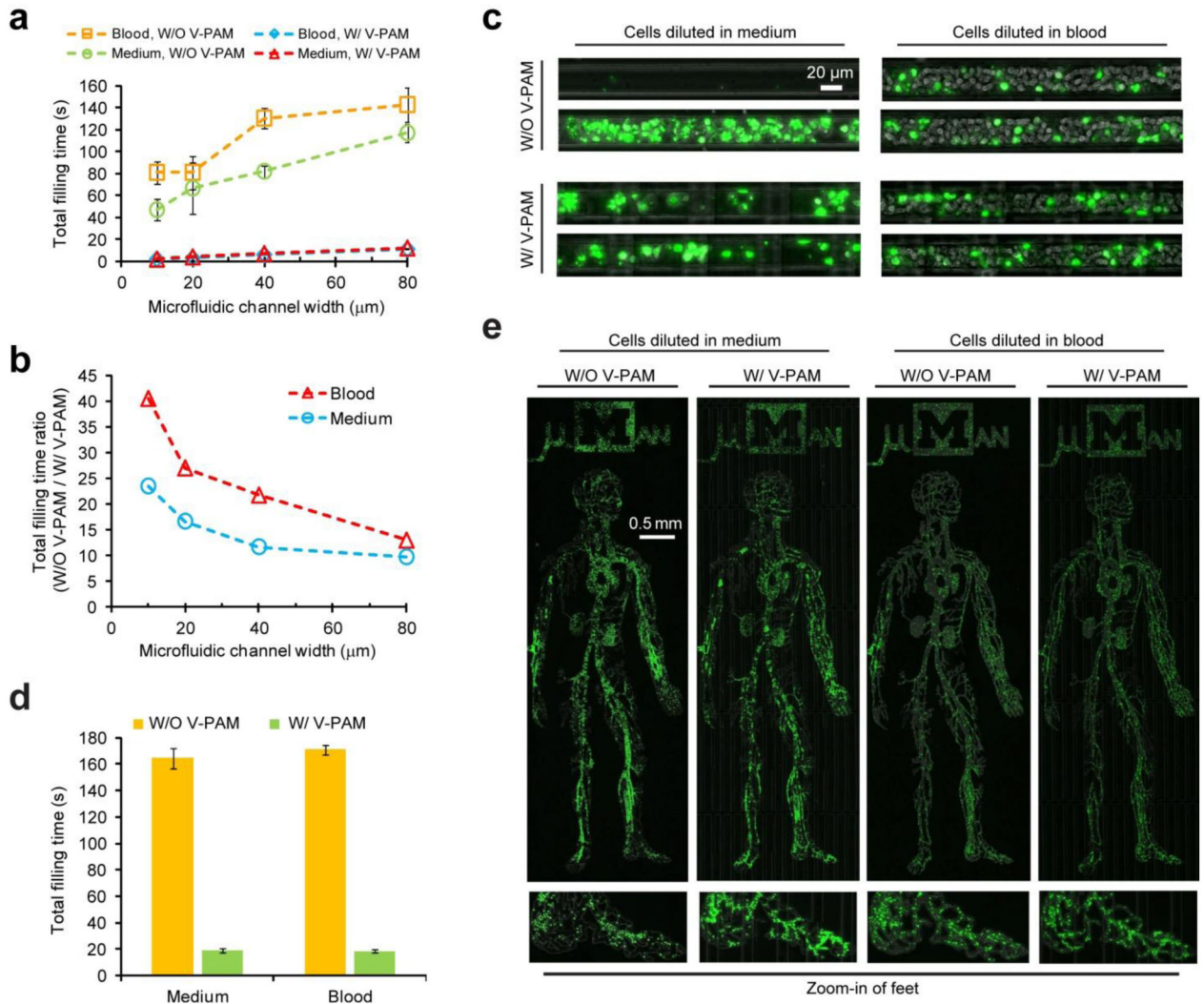
Figure 7.
Rapid filling of complex biofluids (cell suspensions or undiluted human whole blood) in microfluidic geometries with dead-end channels using V-PAM. (**a**) Plot of total filling time as a function of microfluidic channel width for filling cell suspensions in 0.5 cm-long, straight, dead-end microfluidic channels with a cross-section of 20 μm × 20 μm. For V-PAM, *L*: 0.5 cm. (**b**) Ratio of total filling times without V-PAM and with V-PAM plotted against microfluidic channel width. Data was extracted from (**a**). (**c**) Distribution of Hoechst-stained cells inside microfluidic channels after filling with cell suspensions. (**d**) Bar plot of total filling time for both cell suspensions and undiluted human whole blood to fill the μMan chip with or without V-PAM, as indicated. (**e**) Distribution of Hoechst-stained cells inside the μMan chip. Insets at the bottom show magnified views of the foot region. For all cases, microchannels were 20 μm thick, *S*: 1.6 krpm, *P*: 12.5 psi, and *V*: 12.5 psi.